SAR IMAGE DESPECKLING BY COMBINATION OF FRACTIONAL-ORDER TOTAL VARIATION AND NONLOCAL LOW RANK REGULARIZATION

Gao Chen[1], *Gang Li*[1,*], *Yu Liu*[2], *Xiao-Ping Zhang*[3], *Li Zhang*[1]

[1] Department of Electronic Engineering, Tsinghua University, Beijing, China
[2] School of Electronic and Information Engineering, Beihang University, Beijing, China
[3] Department of Electrical & Computer Engineering, Ryerson University, Toronto, Canada

ABSTRACT

This paper proposes a combinational regularization model for synthetic aperture radar (SAR) image despeckling. In contrast to most of the well-known regularization methods that only use one image prior property, the proposed combinational regularization model includes both fractional-order total variation (FrTV) regularization term and nonlocal low rank (NLR) regularization term. By characterizing the smoothness and nonlocal self-similarity property of the SAR image simultaneously, the proposed model, on the one hand, can better remove the noise in homogeneous regions of a noisy image, and on the other hand, can better preserve edges and geometrical features of the images during the despeckling process. Afterwards, an alternating direction method (ADM) is derived to efficiently solve the optimization problem in the proposed model. Experimental results demonstrate the good performance of the proposed model, both in removing SAR image speckles and preserving image texture and details.

***Index Terms*—**SAR image despeckling, fractional-order total variation, nonlocal low rank, alternating direction

1. INTRODUCTION

Despeckling is an important task in synthetic aperture radar (SAR) image processing. The regularization method is an effective tool for SAR image despeckling [1]. In this framework, designing effective regularization terms to describe the image priors plays a vital role. The total variation (TV)-based regularization model [2] is one of the most successful and representative models for additive white Gaussian noise denoising due to its advantage of preserving image edges. In the last decade, this model has been extended to SAR image despeckling, such as the AA model [3], the SO model [4] [5] etc. However, the TV regularized term often favors piecewise constant solution and therefore fails to preserve the textures and often causes staircase effect [6]. In order to improve the ability of texture preservation, a class of non-local fractional-order total variation (FrTV) regularized models has been widely proposed in recent years [7, 8]. Nevertheless, as shown in [9], some point-like and fine structures are still not accurately recovered by the FrTV regularization algorithms. That is because it does not explore nonlocal self-similarities which are common in SAR images.

The nonlocal means (NLM) [10] is an effective method that exploits image self-similarity for image denoising. A series of nonlocal regularization terms for SAR image despeckling were proposed by exploiting the nonlocal self-similarity property of SAR images, such as the probabilistic patch-based (PPB) algorithm [11], the SAR-oriented version of block-matching 3-D (SAR-BM3D) algorithm [12], and the nonlocal framework for SAR denoising (NLSAR) [13] etc. Due to the exploitation of self-similarity prior of SAR images, nonlocal regularization algorithms have better despeckling performance than the local regularization algorithms, with sharper image edges and more image details [14]. However, the images recovered by nonlocal filtering have blocky effect in smooth regions, which is caused by patch-based self-similarity priors.

In this paper, by characterizing the smoothness and nonlocal self-similarity property of the SAR image simultaneously, we propose a combinational regularization model for speckle reduction (CRM-SR). Different from most of the well-known regularization methods that only use one image prior property, the proposed combinational regularization model includes a FrTV regularization term [8] and a nonlocal low rank (NLR) regularization term [15]. The role of the FrTV regularization term is to better preserve the edges and texture details of SAR images, while the NLR term is capable of preserving more geometrical and fine structures of SAR images. An alternating direction method (ADM) [16] [17] is derived to efficiently solve the optimization problem in the proposed model. Experimental results show that the proposed model can effectively remove SAR image speckles and preserve the geometrical features of images according to both subjective visual assessment of image quality and objective evaluation.

* Corresponding author: gangli@mail.tsinghua.edu.cn

The rest of this paper is organized as follows. Section II elaborates on the design of the combinational regularization model for SAR image speckle reduction. Section III proposes the ADM for solving the optimization problem in the proposed model. Experiment results are presented in Section IV. The concluding remarks are given in Section V.

2. COMBINATIONAL REGULARIZATION MODEL FOR SAR IMAGE DESPECKLING

The speckle in SAR images is characterized by the multiplicative noise model [18]:

$$\boldsymbol{f} = \boldsymbol{u}\boldsymbol{n} \tag{1}$$

where $\boldsymbol{u}$ is the noise-free SAR image and $\boldsymbol{n}$ is the speckle noise that can be modeled by a gamma distribution. The purpose of despeckling is to recover $\boldsymbol{u}$ from $\boldsymbol{f}$. Similar to the SO model in [4], here the multiplicative model is transformed into the additive model by logarithmic transformation $\boldsymbol{w} = log\,\boldsymbol{u}$ and the problem of despeckling is converted into recovering $\boldsymbol{w} = log\,\boldsymbol{u}$ from the noisy observation $\log \boldsymbol{f}$.

In the proposed CRM-SR, the data fidelity term is derived by using the maximum *a posteriori* (MAP) estimator for the gamma distribution of the noise, as stated in [4], and the regularization term $\boldsymbol{\Psi}(\boldsymbol{w})$ is elaborately designed to reflect the smoothness and nonlocal self-similarity of SAR image simultaneously. Overall, the despeckling model can be formulated as:

$$\begin{aligned} \widehat{\boldsymbol{w}} &= \min_{\boldsymbol{w}} \sum_{i=1}^{N}\sum_{j=1}^{N}\left(\boldsymbol{w}_{i,j} + \boldsymbol{f}_{i,j}e^{-\boldsymbol{w}_{i,j}}\right) + \lambda \boldsymbol{\Psi}_{LSM}(\boldsymbol{w}) + \xi \boldsymbol{\Psi}_{NLSM}(\boldsymbol{w}) \\ \boldsymbol{u} &= \exp\left(\widehat{\boldsymbol{w}}\right) \end{aligned} \tag{2}$$

where $\boldsymbol{f}$ is the noisy image; $\boldsymbol{\Psi}_{LSM}(\boldsymbol{w})$ and $\boldsymbol{\Psi}_{NLSM}(\boldsymbol{w})$ indicate the image smoothness and nonlocal self-similarity prior information, respectively; λ and ξ are regularization parameters, which controls the trade-off between the two regularization terms. More details on how to design $\boldsymbol{\Psi}_{LSM}(\boldsymbol{w})$ and $\boldsymbol{\Psi}_{NLSM}(\boldsymbol{w})$ to characterize the two properties are given below.

2.1 Fractional-order Total Variation Model for Smoothness Property of Logarithmic SAR Image

FrTV model [8] is exploited to characterize the smoothness property of the logarithmic SAR image. Without loss of generality, let $\boldsymbol{w}_{i,j}$ denote the pixel in the *i-th* row and the *j-th* column of a $N \times N$ logarithmic image $\boldsymbol{w}$, the fractional-order discrete gradient transform is defined in terms of the fractional-order derivatives in the directions of the columns and rows:

$$\left[\nabla^{\alpha}\boldsymbol{w}\right]_{i,j} = \left(\left(\boldsymbol{w}_h^{\alpha}\right)_{i,j}, \left(\boldsymbol{w}_v^{\alpha}\right)_{i,j}\right) \tag{3}$$

where

$$\begin{cases} \left(\boldsymbol{w}_h^{\alpha}\right)_{i,j} = \sum_{k=0}^{K-1} E_k^{(\boldsymbol{\alpha})}\boldsymbol{w}(i-k,j) \\ \left(\boldsymbol{w}_v^{\alpha}\right)_{i,j} = \sum_{k=0}^{K-1} E_k^{(\boldsymbol{\alpha})}\boldsymbol{w}(i,j-k) \end{cases} \tag{4}$$

$$E_k^{(\boldsymbol{\alpha})} = (-1)^k \frac{\Gamma(\alpha+1)}{\Gamma(k+1)\Gamma(\alpha-k+1)} \tag{5}$$

α is the fractional order of the FrTV norm, $\Gamma(x)$ is the Gamma function, $K \geq 3$ is the number of terms involved in the computation of the fractional-order derivative and is usually set as $K = N$. Based on this definition, the FrTV semi-norm is defined as:

$$\boldsymbol{\Psi}_{LSM}(\boldsymbol{w}) = \|\boldsymbol{w}\|_{FrTV} = \sum_{i=1}^{N}\sum_{j=1}^{N}\sqrt{\left[\left(\boldsymbol{w}_h^{\alpha}\right)_{i,j}\right]^2 + \left[\left(\boldsymbol{w}_v^{\alpha}\right)_{i,j}\right]^2} \tag{6}$$

2.2 Nonlocal Low Rank Model for Self-similarity Property of Logarithmic SAR Image

The implementation details of the design of the NLR model to characterize the nonlocal self-similarity property of logarithmic SAR image are given as follows:

1) The image $\boldsymbol{w}$ (of size $N \times N$) is divided into P overlapped blocks $\boldsymbol{w}_l$ with the same size of $n \times n$, $l = 1, \cdots, P$. For each block $\boldsymbol{w}_l$, find c similar patches in a large search range and then stack them together in a group $\boldsymbol{D}_{\boldsymbol{w}_l} \in \mathbb{R}^{n^2 \times c}$.
2) Apply the singular value decomposition (SVD) to the matrix $\boldsymbol{D}_{\boldsymbol{w}_l}$, followed by arranging the singular values of all the image blocks in a lexicographic order to form a new vector denoted as $\boldsymbol{\Theta}_{\boldsymbol{w}}$. Since the matrix $\boldsymbol{D}_{\boldsymbol{w}_l}$ has a low-rank property, $\boldsymbol{\Theta}_{\boldsymbol{w}}$ is a sparse vector. The nuclear norm is used to measure this low-rank property:

$$\boldsymbol{\Psi}_{NLSM}(\boldsymbol{w}) = \|\boldsymbol{\Theta}_{\boldsymbol{w}}\|_0 = \sum_{l=1}^{P}\left\|\boldsymbol{D}_{\boldsymbol{w}^l}\right\|_* = \sum_{l=1}^{P}\left\|\boldsymbol{G}_l(\boldsymbol{w})\right\|_* \tag{7}$$

where $\|\bullet\|_*$ denotes the nuclear norm and

$$\left[\boldsymbol{G}_l(\boldsymbol{w})\right]_{i,j} = \sum_{k=1}^{N^2}\left(\boldsymbol{R}_l^{\,j}\right)_{i,k}\left[vec(\boldsymbol{w})\right]_k = \sum_{ii=1}^{N}\sum_{jj=1}^{N}\left(\boldsymbol{R}_l^{\,j}\right)_{i,(jj-1)N+ii}\boldsymbol{w}_{ii,jj} \tag{8}$$

$\boldsymbol{R}_l^{\,j} \in \mathbb{R}^{n^2 \times N^2}$ is the matrix operator that extracts the *j-th* block from image $\boldsymbol{w}$.

3. ALTERNATING DIRECTION METHOD FOR SAR IMAGE DESPECKLING USING CRM-SR

Note that the objective function in CRM-SR is non-smooth. In this section, we employ the algorithmic framework of the ADM to solve the optimization problem (2) efficiently.

The problem (2) is reformulated into an equivalent problem by introducing some splitting variables as follows:

$$\widehat{\boldsymbol{w}} = \min_{\boldsymbol{w}} \sum_{i=1}^{N}\sum_{j=1}^{N}\left(\boldsymbol{w}_{i,j} + \boldsymbol{f}_{i,j}e^{-\boldsymbol{w}_{i,j}}\right) + \xi\sum_{l=1}^{P}\left\|\boldsymbol{Z}_l\right\|_* + \lambda\left\|\boldsymbol{Z}_{P+1}\right\|_{FrTV}$$
$$s.t.\quad \boldsymbol{Z}_l = \boldsymbol{G}_l(\boldsymbol{w}) \quad (l = 1,\cdots,P) \qquad (9)$$
$$\boldsymbol{Z}_{P+1} = \boldsymbol{w}$$

The augmented Lagrangian function of problem (9) is given by:

$$\begin{aligned} L_A(\boldsymbol{Z}_l, \boldsymbol{w}) = & \sum_{i=1}^{N}\sum_{j=1}^{N}\left(\boldsymbol{w}_{i,j} + \boldsymbol{f}_{i,j}e^{-\boldsymbol{w}_{i,j}}\right) + \xi\sum_{l=1}^{P}\left\|\boldsymbol{Z}_l\right\|_* + \lambda\left\|\boldsymbol{Z}_{P+1}\right\|_{FrTV} \\ & + \sum_{l=1}^{P}\left[\left\langle \boldsymbol{Y}_l, \boldsymbol{Z}_l - \boldsymbol{G}_l(\boldsymbol{w})\right\rangle + \frac{\beta}{2}\left\|\boldsymbol{Z}_l - \boldsymbol{G}_l(\boldsymbol{w})\right\|_F^2\right] \\ & + \left\langle \boldsymbol{Y}_{P+1}, \boldsymbol{Z}_{P+1} - \boldsymbol{w}\right\rangle + \frac{\beta}{2}\left\|\boldsymbol{Z}_{P+1} - \boldsymbol{w}\right\|_F^2 \end{aligned} \qquad (10)$$

where $\langle\bullet\rangle$ denotes the standard trace inner product for the matrix, or the standard inner product for vectors. $\boldsymbol{Y}_l\,(l = 1,\cdots,P+1)$ are the Lagrangian multipliers, and $\beta > 0$ is a penalty parameter.

In each iteration, we optimize $\boldsymbol{Z}_l\,(l = 1,\cdots,P+1)$ and $\boldsymbol{w}$ alternatively with other variables fixed, and the Lagrangian multipliers are updated by the following scheme:

$$\begin{cases} \boldsymbol{Y}_l \leftarrow \boldsymbol{Y}_l + \gamma\beta\left(\boldsymbol{Z}_l - \boldsymbol{G}_l(\boldsymbol{w})\right) & l = 1,\cdots P \\ \boldsymbol{Y}_{P+1} \leftarrow \boldsymbol{Y}_{P+1} + \gamma\beta\left(\boldsymbol{Z}_{P+1} - \boldsymbol{w}\right) \end{cases} \qquad (11)$$

For $\boldsymbol{w}$ optimization sub-problem, it can be reformulated as:

$$\begin{aligned} \boldsymbol{w}^{(k+1)} = \arg\min_{\boldsymbol{w}} & \sum_{i=1}^{N}\sum_{j=1}^{N}\left(\boldsymbol{w}_{i,j} + \boldsymbol{f}_{i,j}e^{-\boldsymbol{w}_{i,j}}\right) \\ & + \sum_{l=1}^{P}\frac{\beta}{2}\left\|\boldsymbol{Z}_l^{(k)} - \boldsymbol{G}_l(\boldsymbol{w}) + \frac{\boldsymbol{Y}_l^{(k)}}{\beta}\right\|_F^2 + \frac{\beta}{2}\left\|\boldsymbol{Z}_{P+1}^{(k)} - \boldsymbol{w} + \frac{\boldsymbol{Y}_{P+1}^{(k)}}{\beta}\right\|_F^2 \end{aligned} \qquad (12)$$

it is a convex quadratic problem and can be solved as follows:

$$\left[F(\boldsymbol{w})\right]_{i,j} = \frac{\partial L_A(\boldsymbol{Z}_l, \boldsymbol{w})}{\partial \boldsymbol{w}_{i,j}} = 1 - \boldsymbol{f}_{i,j}e^{-\boldsymbol{w}_{i,j}} - \boldsymbol{A}_{i,j} - \boldsymbol{B}_{i,j} = 0 \qquad (13)$$

where

$$\boldsymbol{A}_{i,j} = \sum_{l=1}^{P}\sum_{ii=1}^{n^2}\sum_{jj=1}^{c}\beta\left(\left(\boldsymbol{Z}_l^{(k)}\right)_{ii,jj} - \sum_{t=1}^{N}\sum_{s=1}^{N}\left(\boldsymbol{R}_l^{jj}\right)_{ii,(t-1)N+s}\boldsymbol{w}_{t,s} + \frac{\left(\boldsymbol{Y}_i^{(k)}\right)_{ii,jj}}{\beta}\right)\left(\boldsymbol{R}_l^{jj}\right)_{ii,(j-1)N+i} \qquad (14)$$

$$\boldsymbol{B}_{i,j} = \beta\left[\left(\boldsymbol{Z}_{P+1}^{(k)}\right)_{i,j} - \boldsymbol{w}_{i,j} + \left(\frac{\boldsymbol{Y}_{P+1}^{(k)}}{\beta}\right)_{i,j}\right] \qquad (15)$$

The Newton iteration scheme for solving $F(\boldsymbol{w}) = 0$ is given by:

$$\left(\boldsymbol{w}_{i,j}\right)_{n+1} = \left(\boldsymbol{w}_{i,j}\right)_n - \frac{1 - \boldsymbol{f}_{i,j}e^{-\left(\boldsymbol{w}_{i,j}\right)_n} - \boldsymbol{A}_{i,j} - \boldsymbol{B}_{i,j}}{\boldsymbol{f}_{i,j}e^{-\left(\boldsymbol{w}_{i,j}\right)_n} + \sum_{l=1}^{P}\sum_{ii=1}^{n^2}\sum_{jj=1}^{c}\beta\left(\left(\boldsymbol{R}_l^{jj}\right)_{ii,(j-1)N+i}\right)^2 + \beta} \qquad (16)$$

For $\boldsymbol{Z}_l\,(l = 1,\cdots,P)$ optimization sub-problem, it can be reformulated as:

$$\boldsymbol{Z}_l^{(k+1)} = \arg\min_{\boldsymbol{Z}_l}\left\|\boldsymbol{Z}_l\right\|_* + \frac{\beta}{2\xi}\left\|\boldsymbol{Z}_l - \left(\boldsymbol{G}_l\left(\boldsymbol{w}^{(k)}\right) - \frac{\boldsymbol{Y}_l^{(k)}}{\beta}\right)\right\|_F^2 \qquad (17)$$

This is a nuclear norm-regularized least square problem. It can be solved by singular value thresholding (SVT) [19]:

$$\boldsymbol{Z}_l^{(k+1)} = D_{\xi/\beta}\left(\boldsymbol{G}_l\left(\boldsymbol{w}^{(k)}\right) - \frac{\boldsymbol{Y}_l^{(k)}}{\beta}\right) \qquad (18)$$

where $D_\tau(\bullet)$ denotes the SVT operator as follows:

$$D_\tau(\boldsymbol{X}) \triangleq \boldsymbol{U}\bullet diag\left(\max(\sigma - \tau, 0)\right)\bullet\boldsymbol{V}^T \qquad (19)$$

and $\boldsymbol{X} = \boldsymbol{U}\bullet diag(\sigma)\bullet\boldsymbol{V}^T$ is SVD of the input matrix

For $\boldsymbol{Z}_{P+1}$ optimization sub-problem, it can be reformulated as:

$$\boldsymbol{Z}_P^{(k+1)} = \arg\min_{\boldsymbol{Z}_P}\left\|\boldsymbol{Z}_{P+1}\right\|_{FrTV} + \frac{\beta}{2\lambda}\left\|\boldsymbol{Z}_{P+1} - \left(\boldsymbol{w}^{(k)} - \frac{\boldsymbol{Y}_{P+1}^{(k)}}{\beta}\right)\right\|_F^2 \qquad (20)$$

This is a FrTV-regularized least square problem, which can be solved by majorization-minimization (MM) algorithm [20].

4. EXPERIMENTAL RESULTS

In this section, the experimental results are presented to demonstrate the performance of the proposed CRM-SR model. In our implementation, the size of each block is set to be 8×8 with 4-pixel-width between the adjacent blocks, the size of training window for searching matched blocks is set to be 40×40. The experiments are tested on two gray-level real SAR images with size 512×512, they are shown in Fig.1. The white boxes highlight the homogeneous region of interest (ROI), which is used to compute the equivalent number of looks (ENL). For a given homogeneous region $\boldsymbol{X}_{reg}$, the ENL can be computed as [21]:

$$ENL = \left[E\left(\boldsymbol{X}_{reg}\right)\right]^2 \Big/ Var\left(\boldsymbol{X}_{reg}\right) \qquad (21)$$

where $E(\boldsymbol{X}_{reg})$ and $Var(\boldsymbol{X}_{reg})$ denote the mean and the variation of the pixel values in region $\boldsymbol{X}_{reg}$. Larger ENL values indicate stronger speckle rejection. In addition to ENL, a new image quality assessment model (*α'β'* ratio value estimator) [22] is exploited to evaluate the visual quality. This metric takes into account both the speckle reduction in homogeneous areas and the detail preservation.

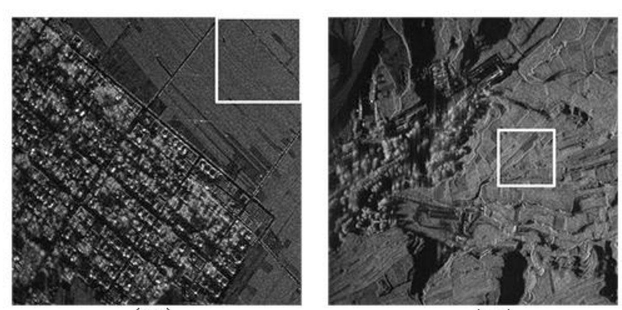

(a) (b)

Fig.1 The real SAR images used in the experiment, the pixels in the white box are used for ENL estimation

Fig.2 Visual quality comparison of the despeckling performances of image Fig.1 (a) using different algorithms

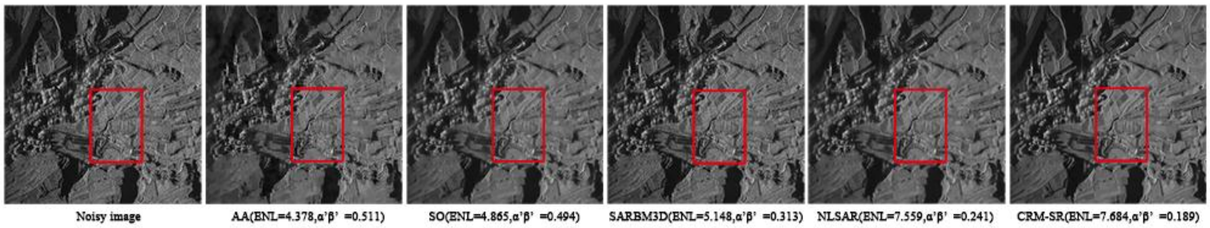

Fig.3 Visual quality comparison of the despeckling performances of image Fig.1 (b) using different algorithms

Unlike the ENL metrics, the smaller *α'β'* ratio value means better visual quality.

In the proposed algorithm, there are several free parameters that need to be set. Parameter α is the fractional order of the FrTV norm. According to the experimental results of [20], α can be selected between $\alpha = 1.2$ and $\alpha = 2$. In our experiments, α is set to be 1.4. In the step of iterative regularization, $\gamma, \beta, N_0, \lambda, \xi$ are set to 1.5, 0.025, 100, 0.045 and 0.27, respectively. These parameters are selected through simulation results.

To demonstrate the performance of the proposed method, we compare the despeckling results with several state-of-the-art SAR image despeckling algorithms, including the AA model [3], the SO model [4], SAR-BM3D algorithm [12] and NLSAR algorithm [13]. For these algorithms, we download the author-provided codes to carry out the despeckling experiments using the default parameters that produce the best performance. Fig.2 and Fig.3 show the despeckling results on the two real SAR images. It can be seen that, the despeckling results of the AA model have a staircase effect and the edges are blurred, especially in Fig.3. The SO model alleviates the staircase effect and achieves better performance in reducing speckle than the AA model, but the despeckled images obtained by the SO model are over-smoothed. SAR-BM3D has the strongest detail-preserving ability. However, its speckle-reduction ability is not good enough, so that there are still some speckles in the images. Besides, it generates some artifacts in flat regions. NLSAR has the strongest speckle-reduction ability. Nevertheless, it loses some details and generates some point-wise artifacts. Compared with the aforementioned methods, the proposed CRM-SR model obtains better despeckling results and preserves the edges and texture details of image effectively by taking the advantages of FrTV and NLR regularization simultaneously.

5. CONCLUSION

In this paper, a novel regularization model for SAR image despeckling is proposed by simultaneously characterizing the two SAR image properties: the smoothness and nonlocal self-similarity. The combination of the FrTV regularization and the NLR regularization produces good despeckling performance and an alternating direction method is derived to solve this combinational regularization model. Experimental results show that the proposed model can effectively remove SAR image speckles and preserve the texture and details of image according to both subjective visual assessment of image quality and objective evaluation.

6. ACKNOWLEDGEMENT

This work was supported in part by the National Natural Science Foundation of China under Grants 61422110 and 61661130158, and in part by the National Ten Thousand Talent Program of China (Young Top-Notch Talent), and in part by the Tsinghua National Laboratory for Information Science (TNList), and in part by the Tsinghua University Initiative Scientific Research Program.

7. REFERENCES

[1] X. S. Ma, H. F. Shen, X. L. Zhao and L. P. Zhang, "SAR image despeckling by the use of variational methods with adaptive nonlocal functionals," *IEEE Transactions on Geoscience and Remote Sensing,* vol. 54, no. 6, pp. 3421-3435, Jun. 2016.

[2] L. I. Rudin, S. Osher and E. Fatemi, "Nonlinear total variation based noise removal algorithms, *Physica D, Nonlinear Phenomena*, vol. 60, no. 1, pp.259-268,1992.

[3] G. Aubert, J. F. Aujol, "A variational approach to removing multiplicative noise," *SIAM Journal on Applied Mathematics,* vol. 68, no. 4, pp. 925-946, 2008.

[4] J. N. Shi and S. Osher, "A nonlinear inverse scale space method for a convex multiplicative noise model," *SIAM Journal on Imaging Sciences*, vol. 1, no. 3, pp. 294-321, 2008.

[5] G. Steidl and T. Teuber, "Removing multiplicative noise by Douglas - Rachford splitting methods," *Journal of Mathematical Imaging and Vision,* vol. 36, no.2 pp. 168-184, 2010.

[6] J. Zhang, Z. H. Wei, and L. Xiao, "A fast adaptive reweighted residual-feedback iterative algorithm for fractional-order total variation regularized multiplicative noise removal of partly-textured images," *Signal Processing*, vol. 98, pp. 381-395, 2014.

[7] J. Bai and X. C. Feng, "Fractional-order anisotropic diffusion for image denoising," *IEEE Transactions on Image Process*ing, vol. 16, no. 10, pp. 2492-2502, Sep. 2007.

[8] D. Tian, Y. K. Du, and D. L. Chen, "An Adaptive fractional-order variation method for multiplicative noise removal," *Journal of Information Science and Engineering*, vol. 32, no. 3, pp.747-762, 2016.

[9] J. Jiang, L. Jiang, and N. Sang, "Non-local sparse models for SAR image despeckling," in *International Conference on Computer Vision in Remote Sensing (CVRS),* Jan.2013, pp. 230-236.

[10] A. Buades, B. Coll, and J. M. Morel, "A non-local algorithm for image denoising," in *IEEE Computer Society Conference on Computer Vision and Pattern Recognition (CVPR),* July 2005, pp. 60-65.

[11] C. Deledalle, L. Denis, and F. Tupin, "Iterative weighted maximum likelihood denoising with probabilistic patch-based weights," *IEEE Transaction on Image Processing.*, vol. 18, no. 12, pp. 2661-2672, Dec. 2009.

[12] S. Parrilli, M. Poderico, C. V. Angelino, and L. Verdoliva, "A nonlocal SAR image denoising algorithm based on LLMMSE wavelet shrinkage," *IEEE Transactions on Geoscience and Remote Sensing*, vol. 50, no. 2, pp. 606-616, Feb. 2012.

[13] C. Deledalle, L. Denis, F. Tupin, A. Reigber, and M. Jager, "NL-SAR: A unified nonlocal framework for resolution-preserving (Pol)(In) SAR denoising," *IEEE Transactions on Geoscience and Remote Sensing*, vol. 53, no. 4, pp. 2021-2038, Apr. 2015.

[14] G. Peyré, "Image processing with nonlocal spectral bases," *Multiscale Modeling & Simulation*, vol. 7, no. 2, pp. 703–730, 2008.

[15] W. Dong, G. Shi, X. Li, Y. Ma, and F. Huang, "Compressive sensing via nonlocal low-rank regularization," *IEEE Trans. Image Process.*, vol. 23, no. 8, pp. 3618–3632, Aug. 2014.

[16] R. Glowinski and P. Le Tallec, *Augmented Lagrangian and Operator Splitting Methods in Nonlinear Mechanics,* Philadelphia, PA: SIAM, 1989.

[17] J. Dong, Z. F. Han, Y. X. Zhao, W. W. Wang, A. Prochazka, and J. Chambers, "Sparse analysis model based multiplicative noise removal with enhanced regularization, " *Signal Process.*, vol.137, pp.160-176, 2017.

[18] C. Oliver and S. Quegan, *Understanding Synthetic Aperture Radar Images With CDROM*, 2nd ed. Raleigh, NC, USA: SciTech, 2004.

[19] E. Cande`s, X. Li, Y. Ma, and J. Wright, "Robust principal component analysis? " *Journal of the ACM,* vol. 58, no. 3, pp. 1-37, 2011.

[20] D. L. Chen, S.S. Sun, C.R. Zhang, Y.Q. Chen and D.Y. Xue, "Fractional-order TV-L2 model for image denoising, " *Central European Journal of Physics,* vol. 11, no. 10, pp. 1414-1422, 2013.

[21] H. Xie, L. E. Pierce, and F. T. Ulaby, "SAR speckle reduction using wavelet denoising and Markov random field modeling, " *IEEE Transactions on Geoscience and Remote Sensing,* vol. 40, no. 10, pp. 2196–2212, Dec. 2002.

[22] L. Gomez, M. E. Buemi, J. C. Jacobo-Berlles, and M. E. Mejail, "A new image quality index for objectively evaluating despeckling filtering in SAR images," *IEEE Journal of Selected Topics in Applied Earth Observations and Remote Sensing*, vol. 9, no. 3, pp. 1297-1307, Mar. 2016.